Synthesis and Structure of a Stable 1,3-Dihydrotriphosphane and Its Thermal Decomposition Leading to the Formation of the Corresponding Phosphine and Diphosphene

Noriyoshi Nagahora, Takahiro Sasamori, Nobuhiro Takeda, and Norihiro Tokitoh*

Institute for Chemical Research, Kyoto University, Gokasho, Uji, Kyoto 611-0011, Japan

Received February 16, 2005

Treatment of dichloroferrocenylphosphine with two molar amounts of a lithium phosphide bearing a 2,4,6-tris[bis(trimethylsilyl)methyl]phenyl (denoted as Tbt) group afforded the corresponding 1,3-dihydro-2-ferrocenyltriphosphane [**1**; $(TbtHP)_2PFc$, Fc = ferrocenyl] as a mixture of three diastereomers in 73% yield. In sharp contrast to the previously reported 1,3-dihydrotriphosphanes [$(RHP)_2PR$, R = Ph, *t*-Bu], **1** was quite stable toward air and moisture either in the solid state or in solution at ambient temperature. The structural characterization of **1** was achieved by NMR spectra and X-ray crystallographic analysis. In the $^{31}P\{^1H\}$ NMR spectrum of the mixture of three diastereomers of **1**, the characteristic two A_2B and one ABX system were observed as signals assignable to two *meso* and one *dl* isomer, respectively. The X-ray crystallographic analysis for a single crystal obtained from the diastereomer mixture of **1** revealed its molecular structure, having P−P bond lengths of 2.2304(12) and 2.2322(12) Å and a P−P−P bond angle of 96.17(5)°, although the configuration could not be determined. Thermolysis of **1** in toluene led to the quantitative formation of $TbtPH_2$ (**2**) and (*E*)-TbtP═PFc (**3**), as judged by the ^1H and ^{31}P NMR spectra. Kinetic studies indicated that the thermolysis of **1** is a first-order reaction including a unimolecular dissociative process, which was reasonablely supported by theoretical calculations.

Introduction

Remarkable progress has been made in the chemistry of open-chain phosphorus compounds because of their unique structures and properties.[1] According to the recent reports of triphosphorus compounds, there were notable candidates for new types of heterocycles as building blocks containing phosphorus atoms[2] and a new class of triphosphane ligands in the field of homogeneous catalysts.[3] Since the first indication for the existence of P_3H_5,[4] which is one of the simple oligophosphorus hydrides, there were numerous reports on the synthesis and characterization of oligo- and polyphosphorus hydrides.[1] In most cases, open-chain phosphorus hydrides are thermally unstable and difficult to treat under ambient temperature due to the weak phosphorus−hydrogen bonds.[5] For example, it was reported by Fehlner in 1968 that P_3H_5 easily underwent thermal decomposition giving PH_3 and P_2H_2 with a first-order kinetic constant to the substrate as speculated by a mass spectrometric study.[6] In addition, 1,3-dihydrotriphosphanes $(RHP)_2PR$ (R = Ph, *t*-Bu) have been reported as marginally stable examples of triphosphorus hydrides (Chart 1).[7,8] $(PhHP)_2PPh$ (**4a**) was found to undergo a disproportionation reaction at room temperature to give homologues of oligophosphorus hydrides $(PhP)_nH_2$ together with cyclic phenylphosphanes $(PhP)_n$ probably via oligomerization of P−H units of **4a**.[7] Similarly, $(t\text{-BuHP})_2P(t\text{-Bu})$ (**4b**) gave a mixture of the corresponding phosphine (t-$BuPH_2$) and cyclotetraphosphetane $(t\text{-BuP})_4$ via its disproportionation reaction.[8] Taking into account that triphosphanes **5a**−**d** (Chart 1), having no phosphorus−hydrogen bond, were isolated as stable compounds,[9] it can be concluded that the

* To whom correspondence should be addressed. Phone: +81-774-38-3200. Fax: +81-774-38-3209. E-mail: tokitoh@boc.kuicr.kyoto-u.ac.jp.

(1) For a review on open-chain phosphorus compounds, see: Baudler, M.; Glinka, K. *Chem. Rev.* **1994**, *94*, 1273−1297.

(2) (a) Breen, T. L.; Stephan, D. W. *Organometallics* **1997**, *16*, 365−369. (b) Bashall, A.; Garcia, F.; Lawson, G. T.; McPartlin, M.; Rothenberger, A.; Woods, A. D.; Wright, D. S. *Can. J. Chem.* **2002**, *80*, 1421−1427. (c) Uhl, W.; Benter, M. *Dalton. Trans.* **2000**, *18*, 3133−3135. (d) Bashall, A.; Hopkins, A. D.; Mays, M. J.; McPartlin, M.; Wood, J. A.; Woods, A. D.; Wright, D. S. *Dalton. Trans.* **2000**, *12*, 1825−1826. (e) Althaus, H.; Breunig, H. J.; Probst, J.; Rösler, R.; Lork, E. *J. Organomet. Chem.* **1999**, *585*, 285−289.

(3) (a) Dou, D.; Duesler, E. N.; Paine, R. T. *Inorg. Chem.* **1999**, *38*, 788−793. (b) Caminade, A. M.; Majoral, J. P.; Mathieu, R. *Chem. Rev.* **1991**, *91*, 575−612, and references therein.

(4) Royen, P.; Hill, K. *Z. Anorg. Allg. Chem.* **1936**, *229*, 97.

(5) Cotton, F. A.; Wilkinson, G.; Murillo, C. A.; Bochmann, M. *Advanced Inorganic Chemistry*, 6th ed.; John Wiley & Sons: Canada, 1999.

(6) Fehlner, T. P. *J. Am. Chem. Soc.* **1966**, *88*, 1819−1821.

(7) (a) Baudler, M.; Koch, D.; Carlsohn, B. *Chem. Ber.* **1978**, *111*, 1217−1220. (b) Baudler, M.; Reuschenbach, G. *Phosphorus Sulfur* **1980**, *9*, 81−85.

(8) (a) Baudler, M.; Hellmann, J.; Reuschenbach, G. *Z. Anorg. Allg. Chem.* **1984**, *509*, 38−52. (b) Baudler, M.; Tschäbunin, H. *Z. Anorg. Allg. Chem.* **1992**, *617*, 31−36.

(9) (a) Bender, H. R. G.; Nieger, M.; Niecke, E. *Z. Naturforsch.* **1993**, *48b*, 1742−1752. (b) Kovacs, I.; Krautscheid, H.; Matern, E.; Sattler, E.; Fritz, G.; Hönle, W.; Borrmann, H.; Schnering, H. G. V. *Z. Anorg. Allg. Chem.* **1996**, *622*, 1564−1572. (c) Urnezius, E.; Lam, K.-C.; Rheingold, A. L.; Protasiewicz, J. D. *J. Organomet. Chem.* **2001**, *630*, 193−197.

10.1021/om0501069 CCC: $30.25
Publication on Web 05/14/2005

Chart 1

$(R^1HP)_2PR^2$

1: R^1 = Tbt, R^2 = Fc
4a: $R^1 = R^2$ = Ph
4b: $R^1 = R^2$ = *t*-Bu

$(R^1{}_2P)_2PR^2$

5a: $R^1 = N(i\text{-}Pr)_2$, $R^2 = SiMe_3$
5b: R^1 = Ph, $R^2 = Si(i\text{-}Pr)_3$
5c: R^1 = *t*-Bu, $R^2 = SiMe_3$
5d: R^1 = Ph, $R^2 = 2,6\text{-}Mes_2C_6H_3$

Tbt:

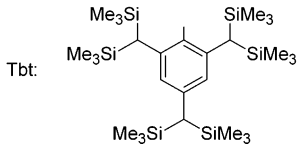

Scheme 1. Synthesis of 1[a]

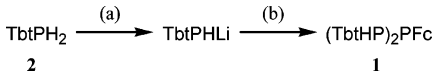

[a] (a) *n*-BuLi (1.0 equiv), Et_2O, −78 °C to rt. (b) $FcPCl_2$ (0.5 equiv), THF, −78 °C to rt.

reactivity of phosphorus−hydrogen bonds inherently gives 1,3-dihydrotriphosphanes thermal instability.

On the other hand, it has been demonstrated by the isolation of Mes*PH_2 (Mes* = 2,4,6-tri-*tert*-butylphenyl) that an aryl-substituted primary phosphine derivative can be easily handled as a stable compound in the open air when it is kinetically well stabilized.[10] In the course of our studies on kinetically stabilized doubly bonded systems between heavier group 15 elements using original steric protection groups, Tbt and 2,6-bis[bis(trimethylsilyl)methyl]-4-[tris(trimethylsilyl)methyl]phenyl (Bbt) groups,[11] we found that the Tbt group is applicable to the kinetic stabilization of 1,3-dihydrotriphosphane $(TbtHP)_2PFc$ (**1**). We report here the synthesis and structure of kinetically stabilized 1,3-dihydrotriphosphane **1**, which can be isolated as a crystalline compound stable at room temperature, together with its unique thermal disproportionation reaction leading to the formation of $TbtPH_2$ (**2**) and (*E*)-TbtP═PFc (**3**).

Results and Discussion

Synthesis and Structural Characterization of 1,3-Dihydrotriphosphane 1. The synthetic route for 1,3-dihydrotriphosphane **1** is shown in Scheme 1. Addition of an Et_2O solution of TbtPHLi[11h] to a THF solution of dichloroferrocenylphosphine[12] at −78 °C gave a diastereomer mixture of **1** as orange crystals in 73% isolated yield. In sharp contrast to the previously reported 1,3-dihydrotriphosphanes **4a**,**b**,[7,8] **1** is stable in the air and on exposure to daylight in the solid state. Moreover, **1** was thermally stable without any decomposition either up to 177 °C in the solid state or at 80 °C in a benzene-d_6 solution in a sealed tube, although **1** has two reactive phosphorus−hydrogen bonds. The remarkable stability of **1** reflects the prominent protecting ability of Tbt groups.

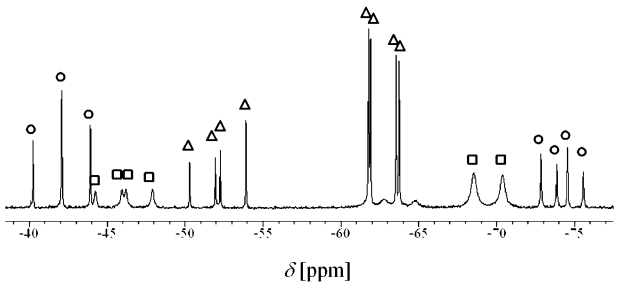

Figure 1. $^{31}P\{^1H\}$ NMR spectrum of **1** in benzene-d_6 at 50 °C. One ABX (open circles) and two A_2B (open triangles and squares) systems were observed.

Chart 2

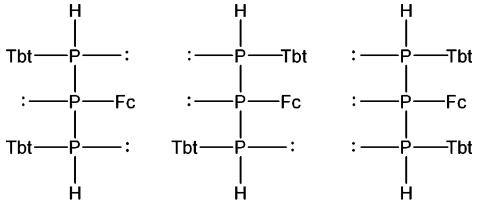

1a (1*S**,3*R**) **1b** (1*R**,3*R**) **1c** (1*R**,3*S**)

Table 1. $^{31}P\{^1H\}$ NMR Data of 1 in Benzene-d_6 at 50 °C

spin system	δ (P^1) [ppm]	δ (P^2) [ppm]	δ (P^3) [ppm]	J_{P1-P2} [Hz]	J_{P1-P3} [Hz]	J_{P2-P3} [Hz]
A_2B	−69.5	−46.2	−69.5	∓221		∓221
ABX	−75.6	−42.2	−73.0	∓223	<±5	∓219
A_2B	−62.6	−52.3	−62.6	∓219		∓219

Compound **1** was isolated as a diastereomeric mixture of **1a** (1*S**,3*R**), **1b** (1*R**,3*R**), and **1c** (1*R**,3*S**) formed in the ratio of 1:1:1, which showed characteristic signals of two A_2B and one ABX system in the $^{31}P\{^1H\}$ NMR spectrum (Chart 2, Figure 1, and Table 1). The two A_2B systems should be assignable to **1a** (1*S**,3*R**) and **1c** (1*R**,3*S**), and the ABX system should be attributed to **1b** (1*R**,3*R**) in analogy with the case of previously reported 1,3-dihydrotriphosphane **4a**.[7,13] It was difficult to draw a final conclusion for the assignment of the two A_2B signals. In the ^1H NMR spectrum for **1**, three singlet signals could be observed separately for the unsubstituted cyclopentadienyl protons of the three diastereomers **1a**−**c** in the ratio 1:1:1, although the full assignment of signals for **1a**−**c** was difficult due to the complexity of the spectrum. Each diastereoisomer of **1a**−**c** could not be separated by using preparative thin-layer, gel permeation liquid chromatography, and recrystallization.

(10) (a) Cowley, A. H.; Kilduff, J. E.; Newman, T. H.; Pakulski, M. *J. Am. Chem. Soc*. **1982**, *104*, 5820−5821. (b) Issleib, K.; Schmidt, H.; Wirkner, C. *Z. Anorg. Allg. Chem*. **1982**, *488*, 75−79. (c) Bertrand, G.; Couret, C.; Escudie, J.; Majid, S.; Majoral, J. P. *Tetrahedron Lett*. **1982**, *23*, 3567−3570. (d) Yoshifuji, M.; Shibayama, K.; Inamoto, N.; Matsushita, T.; Nishimoto, K. *J. Am. Chem. Soc.* **1983**, *105*, 2495−2497.

(11) (a) Tokitoh, N.; Arai, Y.; Okazaki, R.; Nagase, S. *Science* **1997**, *277*, 78−80. (b) Tokitoh, N.; Arai, Y.; Sasamori, T.; Okazaki, R.; Nagase, S.; Uekusa, H.; Ohashi, Y. *J. Am. Chem. Soc*. **1998**, *120*, 433−434. (c) Sasamori, T.; Takeda, N.; Tokitoh, N. *Chem. Commun*. **2000**, 1353−1354. (d) Sasamori, T.; Arai, Y.; Takeda, N.; Okazaki, R.; Furukawa, Y.; Kimura, M.; Nagase, S.; Tokitoh, N. *Bull. Chem. Soc. Jpn*. **2002**, *75*, 661−675. (e) Sasamori, T.; Takeda, N.; Fujio, M.; Kimura, M.; Nagase, S.; Tokitoh, N. *Angew. Chem., Int. Ed*. **2002**, *41*, 139−141. (f) Sasamori, T.; Takeda, N.; Tokitoh, N. *J. Phys. Org. Chem*. **2003**, *16*, 450−462. (g) Sasamori, T.; Mieda, E.; Takeda, N.; Tokitoh, N. *Chem. Lett*. **2004**, *33*, 104−105. (h) Nagahora, N.; Sasamori, T.; Takeda, N.; Tokitoh, N. *Chem. Eur. J*. **2004**, *10*, 6146−6451. (i) Sasamori, T.; Mieda, E.; Nagahora, N.; Takeda, N.; Takagi, N.; Nagase, S.; Tokitoh, N. *Chem. Lett.* **2005**, *34*, 166−167.

(12) Sollott, G. P.; Howard, G. *J. Org. Chem*. **1964**, *29*, 2451−2452.

(13) Baudler, M.; Reuschenbach, G.; Koch, D.; Carlsohn, B. *Chem. Ber*. **1980**, *113*, 1264−1271.

Table 2. Inversion Barriers at a Tricoordinated Phosphorus Atom

molecule	inversion energy [kcal/mol]	reference
PH_3	35	14a
$(H_2P)_2$	26.5	14b
$(PhHP)_2$	22	14c
$(PhMeP)_2$	23.6	14d
$(H_2P)_2PH$	27.3	14a
$(H_2P)_2PH$	20.3	14a
$[Ph(Me_3Si)P]_2PPh$[a]	10−15	13

[a] In this case, the phosphorus atoms at the terminal positions may invert due to the low electronegativity of the silicon atom.

Reported inversion barriers of the phosphorus atom for several types of phosphines shown in Table 2 indicated that the introduction of bulky substituents at the phosphorus atom decreases the inversion barriers.[14] It can be considered that the inversion barrier of **1** should be smaller than those reported for **4a**,**b** due to the extremely bulky substituent, Tbt, and the inversion at the phosphorus atom of **1a**−**c** in solution should give rise to the equilibrium state between **1a**, **1b**, and **1c** under ambient conditions.[15] Therefore, **1** was observed as a mixture of diastereomers **1a**−**c** in the ratio of 1:1:1 in solution at ambient temperature. This is probably due to the small difference in thermodynamic stability between **1a**, **1b**, and **1c**, which was supported by theoretical calculations for the model molecules **6a**−**c** [$(DmpHP)_2PFc$ (Dmp = 2,6-dimethylphenyl)] (Figure 2).[16]

The structural characterization of **4a**,**b** has not been fully accomplished due to their inherent instability,[7,8] and the solid state structures have been known for only four triphosphane derivatives, **5a**−**d**, so far (Chart 1).[9] Taking into account these previous reports, compound **1** is the first example of a kinetically stabilized 1,3-dihydrotriphosphane derivative. Fortunately, single crystals of **1** suitable for X-ray crystallographic analysis were obtained by slow recrystallization of an *n*-hexane solution of **1**. The molecular structure of **1** was determined by X-ray crystallographic analysis (Table 3), and the ORTEP drawing and selected structural parameters are shown in Figure 3 and Table 4, respectively. Since the geometry of the hydrogen atoms on the phosphorus atoms of **1** cannot be determined by the X-ray crystallographic analysis in principle, it was not revealed whether the single crystal might consist of one isomer or contain three isomers, **1a**−**c**. When single crystals of **1** were redissolved in benzene-d_6 solution, the ratio of the diastereomers **1a**−**c** estimated by the ^1H NMR spectrum was 1:1:1, the same as before the crystallization, probably due to the inversion of the phosphorus atoms of **1**. The phosphorus−phosphorus bond lengths of **1** are 2.2304(12) and 2.2322(12) Å, which lie in a range of typical phosphorus−phosphorus single bond lengths (ca. 2.19−2.24 Å)[17] and are comparable to those of previously reported triphosphanes (2.190−2.268 Å).[9] The P−P−P bond angle [96.17(5)°] of **1** is somewhat smaller than those of the reported triphosphanes **5a**−**d** (100.0−118.7°).[9]

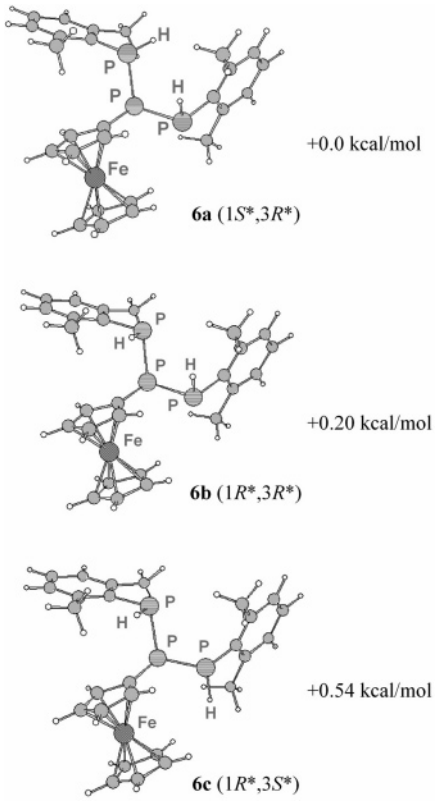

Figure 2. Optimized structures and relative energies of **6a**−**c** calculated at the B3LYP/6-31G(d) level.

Table 3. Crystallographic Data and Experimental Parameters for the Crystal Structure Analysis of 1

formula	$C_{64}H_{129}FeP_3Si_{12}$
fw	1384.51
cryst dimens/mm	0.50 × 0.50 × 0.35
collection temp/K	103(2)
cryst syst	monoclinic
space group	$P2_1/n$ (#14)
a/Å	17.626(4)
b/Å	22.035(5)
c/Å	22.441(5)
β/deg	103.146(3)
volume/Å^3	8487(3)
Z	4
density/Mg m^{-3}	1.084
no. of indep reflns	14 935
no. of params	765
R_1 [$I > 2\sigma(I)$]	0.056
wR_2 (all data)	0.113
goodness of fit	1.095

Thermolysis of 1,3-Dihydrotriphosphane 1. We carried out the thermolysis of **1** in toluene-d_8 to investigate the thermal stability of **1**. Heating of the solution of **1** in a sealed tube at 130 °C afforded both $TbtPH_2$ (**2**)[11h] and (*E*)-TbtP=PFc (**3**)[11h] in the ratio 1:1 as shown

(14) (a) Glukhovtsev, M. N.; Dransfeld, A.; Schleyer, P. v. R. *J. Phys. Chem*. **1996**, *100*, 13447−13454. (b) Rak, J.; Skurski, P.; Liwo, A.; Błażejowski, J. *J. Am. Chem. Soc*. **1995**, *117*, 2638−2648. (c) Albrand, J. P.; Gagnaire, D. *J. Am. Chem. Soc*. **1972**, *94*, 8630−8632. (d) Lambert, J. B.; Jackson, G. F.; Mueller, D. C. *J. Am. Chem. Soc*. **1970**, *92*, 3093−3097.

(15) Since the transition state for the inversion of a tricoordinated phosphorus atom should be considered to have a planar geometry with an sp^2-hybridized phosphorus atom, bulky substituents on the phosphorus atom are known to stabilize the transition state due to the relief of steric repulsion; see: Nagase, S. Structures and Reactions of Compounds Containing Heavier Main Group Elements. In *The Transition State−A Theoretical Approach*, Fueno, T., Ed.; Gordon Science: Amsterdam, 1999; Chapter 8.

(16) $(DmpHP)_2PFc$ **6a**−**c** have optimized structures as (1*S**,3*R**), (1*R**,3*R**), and (1*R**,3*S**) geometries, respectively. In Figure 2 are shown the relative energies for **6a**−**c** calculated at B3LYP/6-31G(d) level.

(17) Baudler, M.; Glinka, K. *Chem. Rev*. **1993**, *93*, 1623−1667, and references therein.

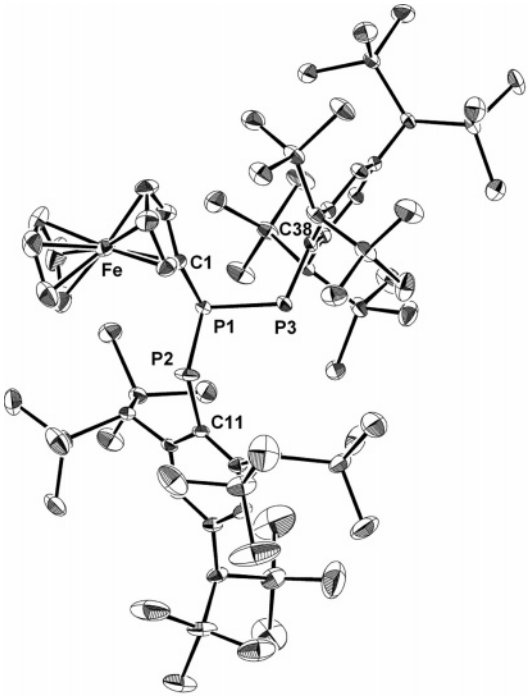

Figure 3. ORTEP drawing of **1** with thermal ellipsoid plots (50% probability). Hydrogen atoms are omitted for clarity.

Table 4. Selected Bond Lengths (Å), Bond Angles (deg), and Torsion Angles (deg) of 1

Bond Lengths	
P(1)−P(2)	2.2322(12)
P(1)−P(3)	2.2304(12)
P(1)−C(1)	1.841(3)
P(2)−C(11)	1.841(3)
P(3)−C(38)	1.845(3)
Bond Angles	
P(2)−P(1)−P(3)	96.17(5)
C(1)−P(1)−P(3)	100.47(11)
C(1)−P(1)−P(2)	95.99(11)
C(11)−P(2)−P(1)	109.61(10)
C(38)−P(3)−P(1)	110.54(10)
Torsion Angles	
C(1)−P(1)−P(2)−C(11)	173.37(15)
C(1)−P(1)−P(3)−C(38)	−70.38(15)
P(2)−P(1)−P(3)−C(38)	−167.66(11)
P(3)−P(1)−P(2)−C(11)	−85.38(12)

Scheme 2. Thermolysis of 1

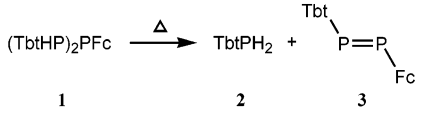

in Scheme 2. The signals for the unsubstituted cyclopentadienyl protons of the three diastereomers **1a**−**c** equally decreased during the thermolysis, as monitored by ^{1}H NMR spectroscopy (Figure 4). In addition, we confirmed that no formation of **1** took place by the reverse reaction of **2** with **3** under the same conditions.

One can see in Figure 5 that plots of a logarithm of the concentration of **1** against time show the linear decay of **1** through >90% consumption in a toluene-d_8 solution at 130 °C, indicating that the thermolysis is a first-order reaction with respect to the concentration of the substrate with the rate constant $k = (6.39 \pm 0.22) \times 10^{-5}$ s^{-1}. The rates of the thermolysis of **1** were

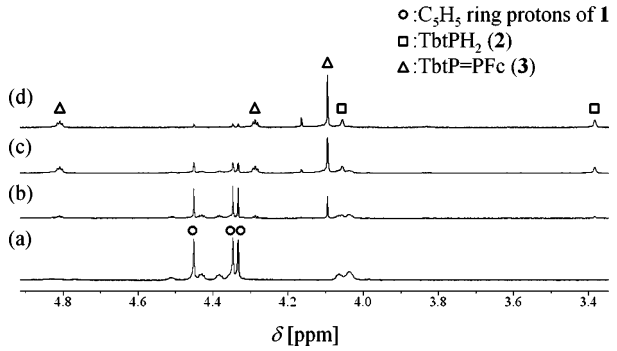

Figure 4. ^{1}H NMR spectral change (3.3−4.9 ppm) for the thermolysis of **1** in toluene-d_8 (a) before heating, (b) after heating at 130 °C for 1.0 h, (c) for 5.0 h, and (d) for 10 h. $TbtPH_2$ (**2**, open squares) and (*E*)-TbtP═PFc (**3**, open triangles) were formed.

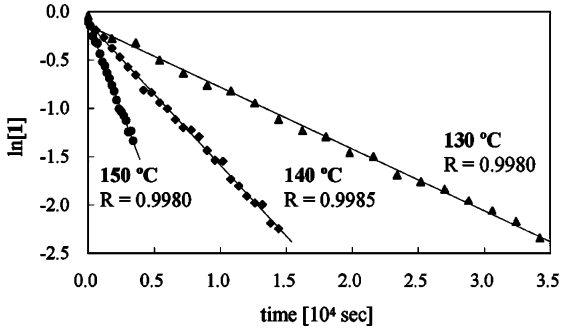

Figure 5. First-order kinetic plots of the thermolysis of **1** in toluene-d_8 (9.95×10^{-3} mol/dm^3) in a range from 130 to 150 °C. The lines are least-squares fit to the data points up to three half-lives.

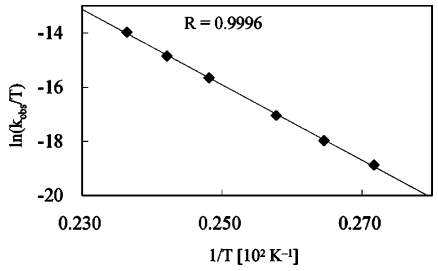

Figure 6. Eyring plot of the thermolysis of **1** in a range from 95 to 150 °C.

Table 5. Data for the Thermal Decomposition of 1 in Toluene-d_8

temperature [°C]	observed kinetic constant [s^{-1}]
95	$(2.34 \pm 0.10) \times 10^{-6}$
105	$(5.89 \pm 0.31) \times 10^{-6}$
115	$(1.54 \pm 0.25) \times 10^{-5}$
130	$(6.39 \pm 0.22) \times 10^{-5}$
140	$(1.47 \pm 0.13) \times 10^{-4}$
150	$(3.68 \pm 0.13) \times 10^{-4}$

monitored at 95, 105, 115, 140, and 150 °C, as summarized in Table 5. The activation parameters were estimated as $\Delta H^{\ddagger} = 28.8 \pm 0.86$ kcal/mol, $\Delta S^{\ddagger} = -6.8 \pm 1.8$ cal/mol·K, and $\Delta G^{\ddagger}(298\ \mathrm{K}) = 30.8 \pm 0.86$ kcal/mol by the Eyring plot shown in Figure 6. These kinetic studies suggested that the thermolysis of **1** should proceed via a unimolecular process with a relatively tight geometry at the transition state.[18]

Kinetic studies on the thermolysis of **1** in a toluene solution were performed using not only NMR but also

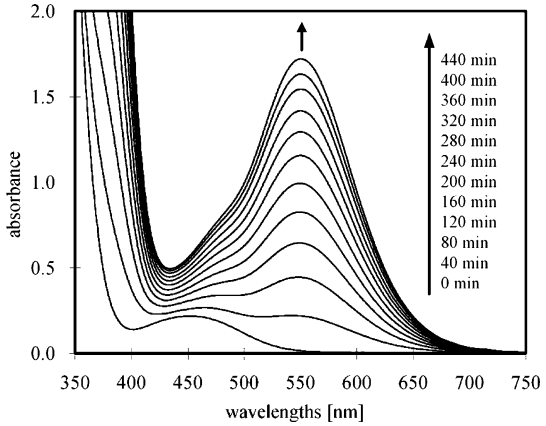

Figure 7. UV/vis spectral change during the thermolysis of **1** in toluene at 130 °C.

Scheme 3. Possible Mechanisms for the Disproportionation Reaction of P_3H_5

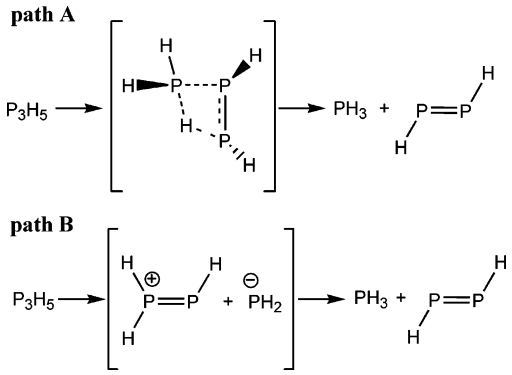

UV/vis spectroscopy. In the UV/vis spectra, the intensities of the metal-to-ligand charge-transfer (MLCT) band for **3** (λ_{max} = 550 nm) were monitored as an index of the concentration of **3** during the heating of a toluene solution of **1** in a sealed quartz cell at 130 °C (Figure 7). The rate constant $k = (5.90 \pm 0.58) \times 10^{-5}$ s^{-1} for the first-order reaction with respect to the concentration of **3** obtained by the UV/vis spectroscopic method was similar to that estimated by the NMR studies.

Theoretical Calculations of P_3H_5. We have performed theoretical calculations on the reaction mechanism for the disproportionation reaction of parent triphosphane P_3H_5 giving PH_3 and (*E*)-HP=PH as a model system. Thus, two different pathways can be postulated for the unimolecular process of the disproportionation reaction of P_3H_5, as shown in Scheme 3.

The first one (path A) is an intramolecular hydrogen-transfer reaction via the transition state with a four-membered ring structure. In the second one (path B), P_3H_5 undergoes a decomposition giving an ionic pair of $P_2H_3^+$ and PH_2^- followed by a proton-transfer reaction leading to the formation of PH_3 and (*E*)-HP=PH. However, a bimolecular route such as path B is inconsistent with the observed negative activation entropy and not suitable as a major mechanistic route. In theoretical calculations, the difference of free energies between P_3H_5 (**7a**) and the ionic pair of $P_2H_3^+$ and PH_2^- was estimated as ΔE = 132 kcal/mol, which was overwhelmingly larger than that between **7a** and **TS7b** (ΔE = 45.2 kcal/mol) (vide infra). We have carried out theoretical calculations on the favorable path A in detail.

In Figure 8 are shown the optimized structure of **7a**, i.e., the most stable conformation of P_3H_5,[19] together with its rotational isomer **7b**, final products **8** and **9**, and their transition states **TS7a** and **TS7b**. The reaction coordinate shown in Figure 9 suggested that the rotational barrier for the phosphorus−phosphorus bond of **7a** giving **7b** was calculated as $\Delta G^{\ddagger}$(298 K) = 3.4 kcal/mol via the transition state **TS7a**. In addition, it was found that **7b** could be converted to PH_3 (**8**) and (*E*)-HP=PH (**9**) via the transition state **TS7b**, having a four-membered ring geometry with a barrier $\Delta G^{\ddagger}$(298 K) = 44.9 kcal/mol. A vector of negative frequency of **TS7b** corresponds to the P1−H5 stretching mode, indicating an intramolecular hydrogen-transfer process giving **8** and **9**. These results suggest that the disproportionation reaction of P_3H_5 giving **8** and **9** is most likely interpreted in terms of an intramolecular hydrogen-transfer process via the four-membered ring transition state **TS7b**.

Reaction Mechanism of 1. Taking into account that the calculated $\Delta S^{\ddagger}$ value (−2.3 cal/mol·K) in the disproportionation process of P_3H_5 is quite consistent with the characteristic negative value of $\Delta S^{\ddagger}$ (−6.8 ± 1.8 cal/mol·K) observed in the thermolysis of **1**, the reaction mechanism of the thermal disproportionation reaction of **1** might be interpreted in terms of the intramolecular hydrogen-transfer process similar to the case of P_3H_5. A possible reaction mechanism is shown in Scheme 4. The three diastereomers **1a** (1*S**,3*R**), **1b** (1*R**,3*R**), and **1c** (1*R**,3*S**) should undergo isomerization to each other (vide supra) due to the ready inversion at the phosphorus atoms under the conditions for the thermolysis of **1**. **TS1a**, **TS1b**, **TS1b′**, and **TS1c** are conceivable as transition states for the intramolecular hydrogen-transfer processes in the thermal disproportionation reaction of **1** based on the theoretical studies described above. In view of the configurations of the transition states, **TS1b′** and **TS1c** giving (*Z*)-TbtP=PFc should not be favored as compared with **TS1a** or **TS1b** due to the steric repulsion between Tbt and Fc groups. Although both **TS1a** and **TS1b** afford (*E*)-TbtP=PFc directly, **TS1b** should be more favorable than **TS1a** because all substituents are placed with an *anti*-configuration in **TS1a**. Consequently, the reaction mechanism of the thermal disproportionation reaction of **1** is most likely interpreted in terms of the pathway from **1b** leading to the formation of **2** and **3** via **TS1b** with a four-membered ring geometry.

Conclusion

In summary, we have succeeded in the synthesis of $(TbtHP)_2PFc$ (**1**) by taking advantage of kinetic stabilization using extremely bulky substituents, Tbt groups.

(18) (a) Li, Y.; Marks, T. J. *Organometallics* **1996**, *15*, 3770−3772. (b) Dexter, C. S.; Hunter, C.; Jackson, F. W. *J. Org. Chem*. **2000**, *65*, 7417−7421. (c) Lin, M.; Spivak, G. J.; Baird, M. C. *Organometallics* **2002**, *21*, 2350−2352. (d) Domínguez, R. M.; Herize, A.; Rotinov, A. Alvarez,-A. A.; Visbal, G. *J. Phys. Org. Chem*. **2004**, *17*, 399−408. (e) Oh, H. K.; Kim, I. K.; Lee, H. W.; Lee, I. *J. Org. Chem*. **2004**, *69*, 3806−3810.

(19) Theoretical investigations for the structures and stabilities of P_3H_5 have been reported. The gauche configuration **7a** with C_s symmetry was found to be the most stable geometry for the P_3H_5 molecule. See: Ding, F. J.; Zhang, L. F. *J. Mol. Struct.* (*THEOCHEM*) **1996**, *369*, 167−172.

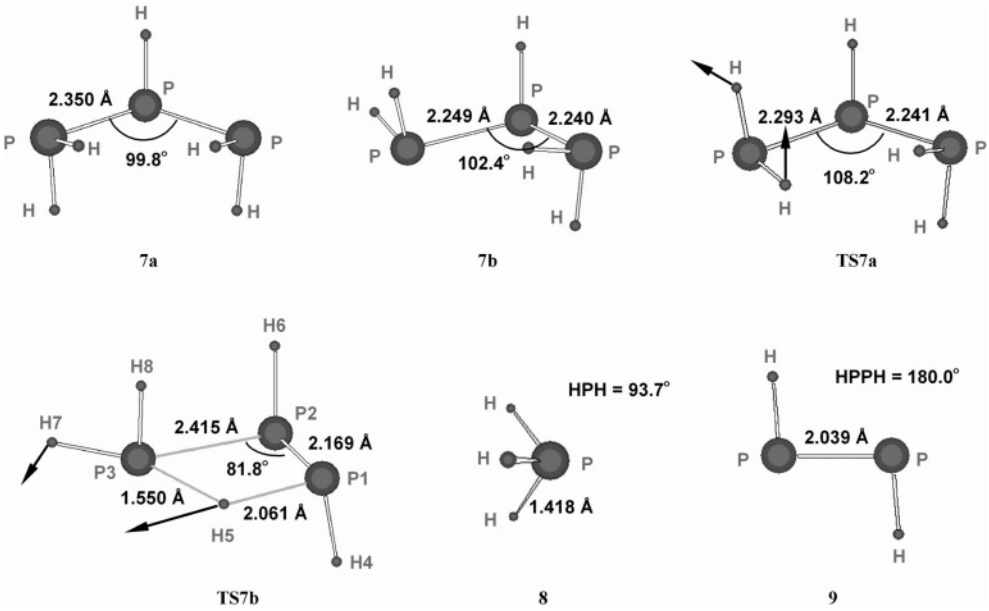

Figure 8. Optimized structures of ground states **7a**, **7b**, **8**, and **9** and transition states **TS7a** and **TS7b** at the B3LYP/6-311+G(2d,p) level. The arrows for **TS7a** and **TS7b** indicate the transition vectors.

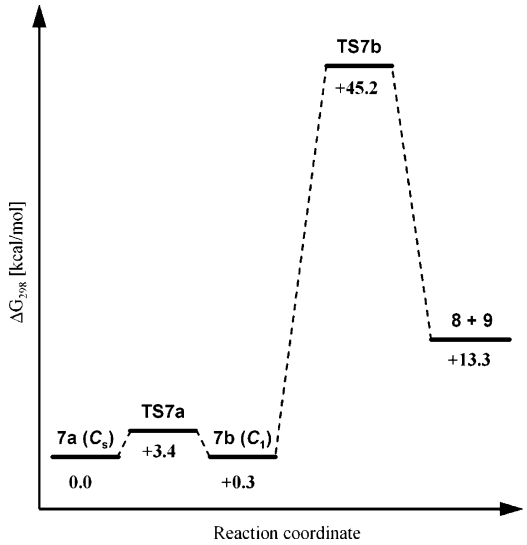

Figure 9. Energy diagram for the disproportionation reaction of P_3H_5 calculated at the B3LYP/6-311+G(2d,p) level. Energies are in kcal/mol (relative to **7a**).

In contrast to the previously reported 1,3-dihydrotriphosphanes [(RHP)$_2$PR, **4a**; R = Ph, **4b**; R = *t*-Bu], **1** was stable in air without any disproportionation at ambient temperature. The structural characterization of **1** was established by the spectroscopic data and X-ray crystallographic analysis. The $^{31}P\{^1H\}$ NMR spectrum for **1** showed two A_2B and one ABX system, which corresponded to two *meso* (**1a** and **1c**) and one *dl* (**1b**) isomer, respectively. The thermolysis of **1** in solution above 95 °C resulted in the quantitative formation of TbtPH$_2$ (**2**) and (*E*)-TbtP=PFc (**3**). The Eyring plot of the thermolysis of **1** in a range from 95 to 150 °C gave the activation parameters $\Delta H^{\ddagger} = 28.8 \pm 0.86$ kcal/mol and $\Delta S^{\ddagger} = -6.8 \pm 1.8$ cal/mol·K as the first-order kinetic constants. The thermal disproportionation reaction of **1** was reasonably interpreted in terms of an intramolecular hydrogen-transfer process via a four-membered ring geometry based on the DFT calculations for the case of P_3H_5. It was found that the existence of hydrogen atoms on the terminal phosphorus atoms of **1** enabled it to undergo the thermal disproportionation reaction. Our studies on the thermolysis of **1** gave a concrete explanation to the previous works on the disproportionation of P_3H_5 by Fehlner.[6] These results may open a door to a new chemistry of open-chain phosphorus hydrides and make it possible to synthesize a new type of diphosphene derivative.

Experimental Section

General Procedures. All reactions were carried out under an argon atmosphere. All solvents were purified by standard methods and then dried by using the Ultimate Solvent System (Glass Contour Company).[20] All solvents (benzene-d_6, toluene-d_8, and toluene) used in the thermolysis of **1** were dried over a potassium mirror before use. Preparative thin-layer chromatography (PTLC) was performed with Merck Kieselgel 60 PF254. Preparative gel permeation liquid chromatography (GPLC) was performed on an LC-908 or LC-918 apparatus equipped with JAI-gel 1H and 2H columns (Japan Analytical Industry Co., Ltd.) with toluene as an eluent. The ^1H NMR (300 MHz) spectra were measured in C_6D_6 or C_7D_8 with a JEOL AL-300 spectrometer using C_6HD_5 (δ = 7.15 ppm) or $C_6D_5CHD_2$ (δ = 2.09 ppm) as an internal standard. $^{31}P\{^1H\}$ NMR (120 MHz) spectra were measured using 85% H_3PO_4 in water (δ = 0 ppm) as an external standard. High-resolution mass spectral data were obtained on a JEOL SX-270 mass spectrometer. The electronic spectra were recorded on a JASCO V-570 UV/vis spectrometer. An oil bath used in the kinetic studies was a LAUDA thermostat K6 KS, the temperature of which was maintained in a range of ±0.2 °C. All melting points were determined on a Yanaco micro melting point apparatus and were uncorrected. Elemental analyses were performed by the Microanalytical Laboratory of the Institute for Chemical Research, Kyoto University. TbtPH$_2$ (**2**)[11h] and dichloroferrocenylphosphine[12] were prepared according to the reported procedures.

Synthesis of 1,3-Dihydrotriphosphane 1. To a solution of TbtPH$_2$ (**2**; 234.1 mg, 0.400 mmol) in ether (10 mL) was added *n*-butyllithium in *n*-hexane (1.50 M, 267 μL, 0.401 mmol) at −78 °C. The solution of TbtPHLi obtained here was

(20) Pangborn, A. B.; Giardello, M. A.; Grubbs, R. H.; Rosen, R. K.; Timmers, F. J. *Organometallics* **1996**, *15*, 1518−1520.

Scheme 4. Possible Mechanism for the Thermolysis of 1

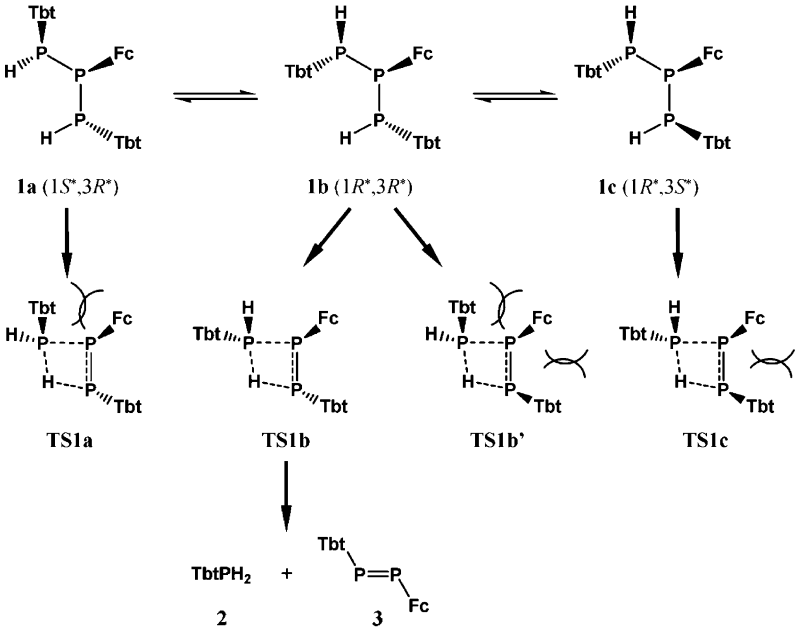

warmed to room temperature for 0.5 h and then cooled to −78 °C. A solution of dichloroferrocenylphosphine (57.4 mg, 0.200 mmol) in ether (10 mL) was added to the reaction mixture at −78 °C. After stirring at the same temperature for 0.5 h, the solution was allowed to warm to room temperature for 6 h. After removal of the solvent, *n*-hexane was added to the residue and the mixture was filtered through Celite. The filtrate was purified by GPLC and PTLC (eluting with *n*-hexane) to afford $(TbtHP)_2PFc$ (**1**; 200.5 mg, 0.145 mmol, 73% yield) as yellow crystals containing three diastereomers, **1a**−**c**. $^{31}P\{^1H\}$ NMR (121 MHz, C_6D_6, 50 °C): δ −75.6, −73.0, −42.2 (ABX system, $^1J_{PP}$ = 223, 219 Hz), −69.5, −46.2 (A_2B system, $^1J_{PP}$ = 221 Hz), −62.6, −52.3 (A_2B system, $^1J_{PP}$ = 219 Hz). HRMS (FAB): found *m/z* 1383.5906 ($[M + H]^+$), calcd for $C_{64}H_{130}FeP_3Si_{12}$ 1383.5956. Anal. Found: C, 55.54; H, 9.49. Calcd for $C_{64}H_{129}FeP_3Si_{12}$: C, 55.52; H, 9.39.

General Procedure for the Kinetic Studies on the Thermolysis of 1. In a glovebox filled with argon, **1** (55.0 mg, 39.8 μmol) was dissolved in dried toluene-d_8 (4.00 mL), and a 600 μL portion of the solution (9.95×10^{-3} mol/dm^3) was transferred to an NMR tube. The tube was degassed and sealed after three freeze−pump−thaw cycles. The sealed tube was heated to 130.0 °C in an oil bath controlled in an error range of ±0.2 °C. The thermolysis was interrupted by cooling to room temperature after regular time intervals to measure the ^1H NMR spectra for over three half-lives. The concentrations of **1a**, **1b**, **1c**, and **3** were determined by the integrals of the corresponding unsubstituted cyclopentadienyl ring protons in the ^1H NMR spectra.

X-ray Crystallographic Analysis of 1. Single crystals of **1** were obtained by slow crystallization from an *n*-hexane solution at room temperature. The intensity data were collected on a Rigaku Mercury CCD diffractometer with graphite-monochromated Mo Kα radiation (λ = 0.71070 Å). The structure was solved by direct methods (SHELXS-97)[21] and refined by full-matrix least-squares procedures on F^2 for all reflections (SHELXL-97).[22] All non-hydrogen atoms were refined anisotropically. All hydrogen atoms except for those on phosphorus atoms were placed using AFIX instructions. No hydrogen atoms on phosphorus atoms were placed. Crystallographic data for **1** are shown in Table 3.

Theoretical Calculations. All theoretical calculations were carried out using the Gaussian 98 program package[23] with density function theory at the B3LYP level. In calculations for **6a**−**c**, the 6-31G(d) basis sets were used. It was confirmed that the optimized structures have minimum energies by frequency calculations. In calculations for P_3H_5, all geometries were fully optimized at the B3LYP/6-311+G(2d,p) level, and it was confirmed by frequency calculations that the optimized structures have minimum energies and the transition state has one imaginary frequency corresponding to the expected transition vectors. Energies and thermodynamic parameters at 298 K were calculated at the same level as structural optimization. The reaction paths were established by the connectivity between the reactant and the transition state by IRC calculations. Computation time was provided by the Supercomputer Laboratory, Institute for Chemical Research, Kyoto University.

Acknowledgment. This work was partially supported by Grants-in-Aid for Scientific Research (Nos. 14078213 and 16750033) and COE Research on "Elements Science" (No. 12COE2005), and the 21st Century COE Program on Kyoto University Alliance for Chemistry from the Ministry of Education, Culture, Sports, Science and Technology, Japan. N.N. thanks Research Fellowships of the Japan Society for the Promotion of Science for Young Scientists.

Supporting Information Available: Theoretically optimized coordinates of **6a**−**c**, **7a**, **7b**, **TS7a**, **TS7b**, **8**, and **9** in PDF format. X-ray crystallographic file of **1** in CIF format. This material is available free of charge via the Internet at http://pubs.acs.org.

OM0501069

(21) Sheldrick, G. M. *Acta Crystallogr. Sect. A* **1990**, *46*, 467−473.
(22) Sheldrick, G. M. *SHELXL-97*, Program for the Refinement of Crystal Structures; University of Göttingen: Göttingen, 1997.
(23) Frisch, M. J.; Trucks, G. W.; Schlegel, H. B.; Scuseria, G. E.; Robb, M. A.; Cheeseman, J. R.; Zakrzewski, V. G.; Montgomery, Jr. J. A.; Stratmann, R. E.; Burant, J. C.; Dapprich, S.; Millam, J. M.; Daniels, A. D.; Kudin, K. N.; Strain, M. C.; Farkas, O.; Tomasi, J.; Barone, V.; Cossi, M.; Cammi, R.; Mennucci, B.; Pomelli, C.; Adamo, C.; Clifford, S.; Ochterski, J.; Petersson, G. A.; Ayala, P. Y.; Cui, Q.; Morokuma, K.; Salvador, P.; Dannenberg, J. J.; Malick, D. K.; Rabuck, A. D.; Raghavachari, K.; Foresman, J. B.; Cioslowski, J.; Ortiz, J. V.; Baboul, A. G.; Stefanov, B. B.; Liu, G.; Liashenko, A.; Piskorz, P.; Komaromi, I.; Gomperts, R.; Martin, R. L.; Fox, D. J.; Keith, T.; Al-Laham, M. A.; Peng, C. Y.; Nanayakkara, A.; Challacombe, M.; Gill, P. M. W.; Johnson, B.; Chen, W.; Wong, M. W.; Andres, J. L.; Gonzalez, C.; Head-Gordon, M.; Replogle, E. S.; Pople, J. A. *Gaussian 98*, Revision A.11; Gaussian, Inc.: Pittsburgh, PA, 2001.